Two- and three-dimensional growth of Bi on *i*-Al-Pd-Mn studied using medium-energy ion scattering

T. C. Q. Noakes* and P. Bailey
STFC Daresbury Laboratory, Daresbury, Warrington WA4 4AD, United Kingdom

C. F. McConville, M. Draxler, M. Walker, M. G. Brown, A. Hentz, and D. P. Woodruff
Department of Physics, University of Warwick, Coventry CV4 7AL, United Kingdom

T. A. Lograsso and A. R. Ross
Ames Laboratory, Iowa State University, Ames, Iowa 50011, USA

J. A. Smerdon, L. Leung, and R. McGrath
Surface Science Research Centre, University of Liverpool, Liverpool L69 3BX, United Kingdom
(Received 29 March 2010; revised manuscript received 16 August 2010; published 9 November 2010)

Recent work on the growth of thin metal films on quasicrystalline substrates has indicated the formation of so-called "magic height" islands with multiples of 4 atomic layers (AL) arising as a result of quantum size effects, which lead to enhanced stability. Here the results of a study are reported of Bi deposition on *i*-Al-Pd-Mn using medium-energy ion scattering to characterize the island thickness and the structural arrangement of Bi atoms within the islands. In addition, data were taken from annealed surfaces after Bi cluster desorption to leave a single aperiodic monolayer of Bi at the surface. Scattered-ion energy spectra from the Bi islands are consistent with a single Bi monolayer covered with mainly 4 AL islands for both 1.8 and 3.2 monolayer equivalent coverages but with some occupation of 2 and 8 Al islands as well. The angular dependence of the scattered-ion intensity ("blocking curve") from Bi has been compared with simulations for various models of both rhombohedral Bi and a distorted "black-phosphorus"-like structure. The data demonstrate bilayer formation within the Bi islands. In the case of the aperiodic Bi monolayer, the blocking curves from substrate scattering are found to be inconsistent with two high-symmetry sites on the quasicrystalline surface that theory indicates are energetically favorable but do not exclude the formation of pentagonal arrangements of Bi atoms as seen in other recent experimental work.

DOI: 10.1103/PhysRevB.82.195418 PACS number(s): 61.44.Br, 61.05.Np, 68.49.Sf, 68.55.J−

I. INTRODUCTION

Recently, surface and interface research in the area of quasiperiodic materials has focused on the use of these materials as substrates for the growth of thin metallic films.[1,2] This interest has been stimulated by the wide range of structural and electronic properties that have been observed in these systems. Studies have ranged from very low coverage to investigate nucleation,[3,4] through monolayer films,[5,6] up to coverages of several monolayers.[7–10]

The work reported here concerns the deposition of Bi onto the fivefold surface of *i*-$Al_{71}Pd_{20}Mn_9$. This system has been the subject of several previous papers, including theoretical work and experimental studies with Bi coverages ranging from submonolayer to multilayer. Also, there are several relevant publications which deal with related systems that can provide additional insight into the various processes occurring across the coverage range.

A theoretical study of the adsorption of Bi on *i*-$Al_{71}Pd_{20}Mn_9$ using density-functional calculations investigated the energetic stability of many different adsorption sites on the surface. Preferred sites included surface vacancies, above Mn atoms, and at the vertices of a P1 Penrose tiling superimposed on the surface structure.[11] Neither vacancy sites nor atop Mn sites were considered to be numerous enough to play an important role in the formation of higher coverage structures. A quasiperiodic monolayer structure was proposed having Bi atoms at the vertices and mid-edge positions of the P1 tiling with the remainder of Bi atoms present as both isolated atoms and pentagonal arrays inside the tiles. In a final step, the positions of the adsorbed Bi atoms were allowed to relax, taking into account the interatomic forces between them and significant movement of many of the atoms in edge and pentagonal sites occurred.[11,12]

A recent study of the nucleation and growth of Bi on *i*-$Al_{71}Pd_{20}Mn_9$ using scanning tunneling microscopy (STM) has shown that growth proceeds via the formation of quasiperiodically ordered pentagonal clusters of atoms, where the edge size of the pentagon is slightly larger (4.9 Å) than that suggested in the theoretical studies. In addition, of the two different orientations of pentagon seen in a P1 tiling, only one was preferred, which appeared to be related to the presence of a central Mn atom in the substrate below. At higher coverages (above 0.5 ML) it was proposed that the additional Bi atoms fill the area between the pentagons but the precise positions could not be established since atomic resolution was lost in the STM images.[13]

At the monolayer deposition level, a study using low-energy electron diffraction (LEED) and helium atom diffraction (HAS) of both Bi and Sb on the fivefold surface of *i*-$Al_{71}Pd_{20}Mn_9$ and on the tenfold surface of *d*-$Al_{72}Ni_{11}Co_{17}$, indicated the formation of pseudomorphic films at 300 °C.

These monolayer films showed little change in the LEED pattern compared to the clean surface, and exhibited atomic densities matching that of Al atoms in the substrate surface. HAS, which is even more surface sensitive, also confirmed the quasiperiodic nature of the adlayers and indicated a high level of ordering in the films, suggesting that a large proportion of the adatoms sit in well-defined sites.[5] Similar results have also been seen for the deposition of Sn on fivefold i-$Al_{63}Cu_{24}Fe_{13}$ at the same substrate temperature. In this case, STM images of the monolayer film show pentagonal features in two orientations, giving rise to tenfold symmetry.[6]

So far there has been only one previous report dealing with higher coverages of Bi on i-$Al_{71}Pd_{20}Mn_9$.[14] In this study, which also employed the technique of STM, Bi deposited at room temperature was seen to form islands above the monolayer film with heights consistent with four rhombohedral [110] layers. This result is essentially identical to the earlier discovery of a preference for islands of height 4 atomic layers (AL) (and multiples thereof) when Bi is deposited on i-$Al_{63}Cu_{24}Fe_{13}$ (and Ag on i-$Al_{71}Pd_{20}Mn_9$).[15] The preference for 4 AL high islands was attributed to quantum size effects, where islands of specific height gain stability from the energetic location of the associated quantum well states. These effects are typically seen for metal overlayers on semiconducting substrates, where the quantum well states lie just below the Fermi level of the metal, and in the band gap of the substrate to ensure quantum confinement. Later work concerning thin films of Ag on d-$Al_{72}Ni_{11}Co_{17}$ and i-$Al_{71}Pd_{20}Mn_9$ demonstrated the presence of quantum well states in these systems but also indicated that the quantum confinement was not due to the low density of states at the Fermi level seen in quasicrystalline materials (the so-called pseudogap), but rather due to the incompatibility of the substrate and overlayer symmetries which preclude electronic coupling.[16]

Although the quantum size effects provide a good explanation of the preference for 4 AL high islands seen for Bi on i-$Al_{71}Pd_{20}Mn_9$ and related systems, there is another potential explanation which comes from work carried out on the closely related system of Bi films grown on Si(111).[17,18] In this system, as with growth on quasicrystalline surfaces, a monolayer film of Bi is seen to form, on top of which Bi islands of 4 AL height grow, as demonstrated by STM studies. However, in this case density-functional theory calculations indicated the formation of a puckered "black-phosphorus"-like structure composed of bilayers of Bi atoms. This bilayer structure would clearly lead to a preference for islands with an even number of atomic layers.

Therefore there are clearly several open questions and discrepancies between theory and experiment concerning both the structure of the aperiodic monolayer and the Bi islands. In this paper, we report the results of a medium-energy ion scattering (MEIS) study of this system. MEIS provides information not only about crystallographic structure of surfaces, thin films and islands, but also (via its composition and depth sensitivity) about island heights and coverages. The technique is fully quantitative in contrast to the previous analyses that were qualitative or at best semiquantitative.

II. EXPERIMENTAL DETAILS

The experiments were conducted at the UK MEIS facility at STFC Daresbury laboratory.[19] The facility comprises an ion source and beamline, capable of delivering a well-defined beam of ions to an experimental endstation housing an analysis chamber, together with additional chambers for sample preparation, storage, and fast entry into the UHV system. The collimated beam of ions enters the analysis chamber, and after passing through a beam current monitor, is incident on the sample mounted on a six-axis goniometer that allows precise alignment of the sample with the beam. The ions scattered from the sample are collected in the horizontal scattering plane by a toroidal electrostatic analyzer equipped with a position sensitive detector. The analyzer disperses the ions in energy, while preserving the angular distribution, and the position sensitive detector can therefore measure simultaneously a range of scattered-ion energies and angles. Several such two-dimensional (2D) data sets can be collected and joined electronically to produce larger scattered-ion intensity maps as a function of angle and energy. Further processing of these two-dimensional data allows both scattered-ion energy plots at fixed scattering angle and scattered-ion angular plots (so-called "blocking curves") for scattering from individual atomic species (identified by their recoil energy loss) to be extracted. The scattered-ion energy plots reveal the depth-dependent composition (and island height distribution) while the blocking curves (angular plots) contain elemental and depth-dependent structural information.

The i-$Al_{70}Pd_{21}Mn_9$ sample was prepared at the Ames laboratory using the Bridgman growth technique, oriented by Laue x-ray diffraction, and cut by spark erosion to obtain a fivefold surface. The surface was polished using progressively smaller particle size diamond paste to a final size of $\frac{1}{4}\mu$m before cleaning in UHV using cycles of ion bombardment (1.5 keV Ar^+, 6 μA, 45° incidence) and annealing (e-beam heating to 620 °C measured using a pyrometer, 1–4 h). The clean surface was prepared using a cumulative anneal time of 19 h, as has previously been found to be required to produce a well-ordered flat surface.[20] Surface ordering and cleanliness were monitored using LEED and Auger electron spectroscopy in the preparation chamber. Bi deposition was carried out using a miniature K cell at 590 °C. The 1.0 ML surface was prepared by depositing for 20 min with the sample held at 300 °C to ensure both that excess Bi would desorb and that the monolayer film would be well ordered. The higher coverage films were deposited onto the substrate at room temperature using times of 12 and 20 min to achieve nominal average coverages of 1.8 monolayer equivalent (MLE) and 3.2 MLE. The base pressure in the UHV chambers used was 2×10^{-10} mbar, and this did not rise to greater than 5×10^{-9} mbar during Bi deposition. The prepared samples were transferred under UHV to the analysis chamber for data collection.

MEIS analysis was carried out using 100 keV He^+ ions, mainly incident in a direction with twofold symmetry at 31.8° from the fivefold surface normal (one of five such equivalent directions). Although not shown here, some data were also collected in a threefold symmetric direction at

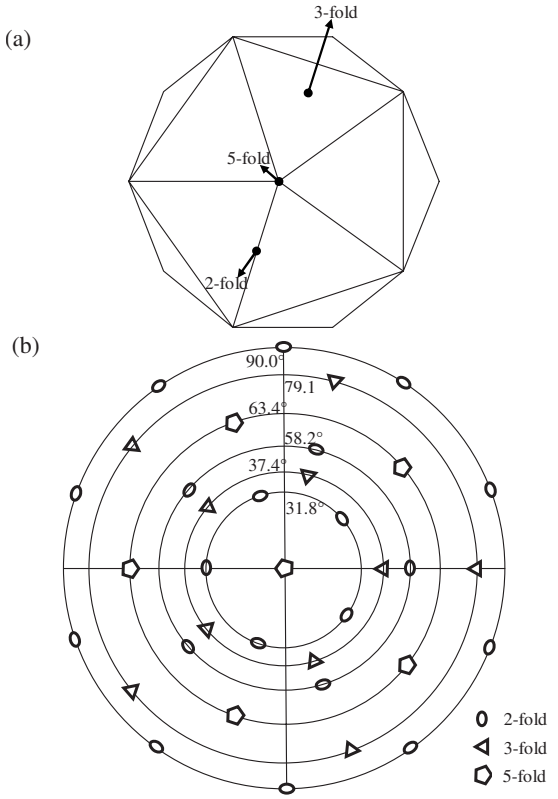

FIG. 1. (a) An icosahedron with twofold, threefold, and fivefold axes indicated. (b) A stereographic projection showing the relative positions of twofold, threefold, and fivefold axes to the fivefold surface. The twofold axis at 31.8° and the twofold axis at 58.2° rotated by 180° azimuthally, effectively define the 90° blocking dip seen in Fig. 2.

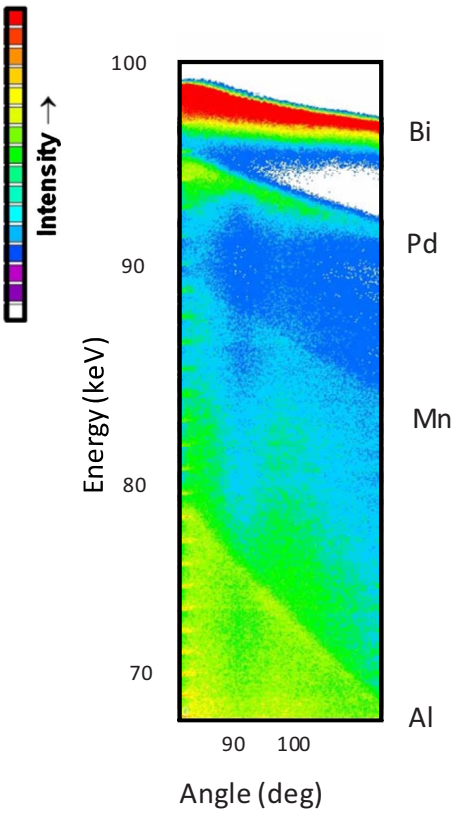

FIG. 2. (Color online) A "2D" plot of scattered-ion intensity (shown by color) versus scattering angle and energy for Bi deposited on *i*-Al-Pd-Mn (3.2 MLE). The features arising from each elemental component can be seen, along with a vertical strip of reduced intensity at 90° scattering arising from a blocking dip in the quasicrystalline substrate.

37.4° from the surface normal but rotated azimuthally by 180° (again one of five equivalent directions). Figure 1 contains a diagram of an icosahedron and an associated stereographic projection indicating the positions of the various axes in terms of incident and azimuthal angle. Data were collected for a range of scattering angles (defined as the angle of in-plane deflection from the direction of the incident beam). Each individual data set was collected for a beam dose of 2.5×10^{15} ions/cm^2 and the sample moved regularly to a fresh part of the surface to minimize beam damage.

III. RESULTS

Figure 2 shows a two-dimensional MEIS ion-energy/angle map obtained from a Bi-deposited *i*-Al-Pd-Mn surface (in this case for 3.2 MLE). Diagonal stripes of enhanced scattered-ion intensity, corresponding to scattering from each of the elemental components having different atomic mass, can be clearly seen. In addition, there are vertical stripes of low-scattering intensity at constant scattering angle that arise due to blocking of outgoing ions by the near-surface atoms of the sample. Figure 3 shows a scattered-ion energy plot obtained by integrating the counts at each energy over a narrow angular range around one of these blocking directions. In addition to the highest-energy peak, corresponding to scattering from the (highest-mass) Bi atoms, there are surface peaks corresponding to scattering from the three elemental components of the substrate. The figure also shows a fit to this energy spectrum using the SIMNRA program,[21] although a good fit of the Bi signal could not be easily achieved for the higher coverages because the software is not designed for

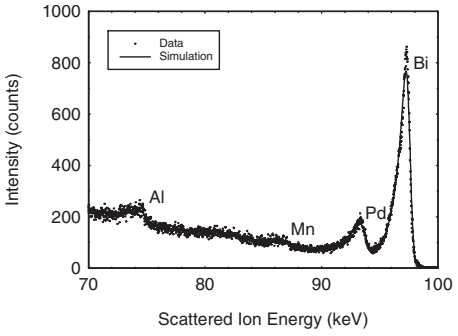

FIG. 3. Energy plot from 3.2 MLE Bi on *i*-Al-Pd-Mn fitted using SIMNRA. The data is extracted by integrating a 0.74° angular range within the 90° blocking dip seen in Fig. 2. The fit to the Bi peak is suboptimal because the software is not ideal for fitting islanded surfaces. The near-surface composition of the substrate is essentially bulklike and there is a slight enhancement of Pd in the topmost layers.

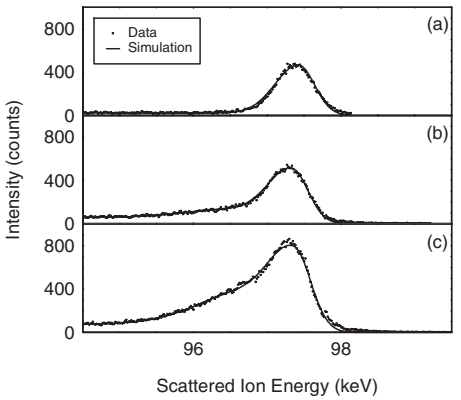

FIG. 4. Detailed energy plots for the Bi intensity for (a) 1 MLE Bi, (b) 1.8 MLE Bi, and (c) 3.2 MLE Bi. The data have been fitted using a proprietary simulation code taking into account the islanded nature of the samples.

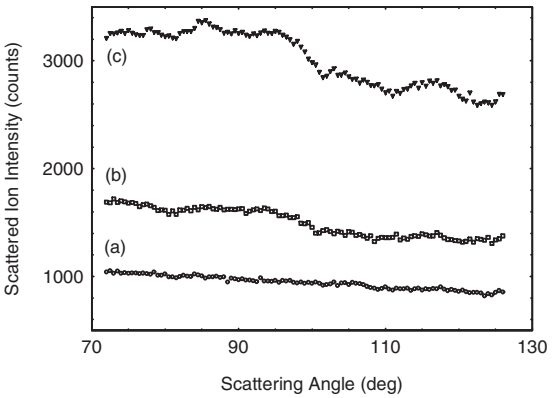

FIG. 5. A plot of the angular dependence of the scattered-ion intensity from Bi for (a) 1 MLE Bi, (b) 1.8 MLE Bi, and (c) 3.2 MLE Bi. The ion beam is aligned with a twofold direction at 31.8° from the surface normal and the in-plane scattering shown over a range of exit angles. The 1 MLE data are essentially featureless whereas with increasing coverage distinct features appear.

use with islanded materials. The fitting parameters used to obtain the simulated spectra provide information on the surface and near-surface composition of the substrate. In these experiments they showed that the composition of the near surface did not vary significantly from the bulk composition (70% Al, 21% Pd, and 9% Mn), apart from an expected slight enhancement of the Pd composition in the topmost layers.[22]

Figure 4 shows, on an expanded energy scale, the peak in the scattered-ion energy spectra corresponding to scattering from Bi recorded from the Bi-covered surfaces with average coverages of 1.0, 1.8, and 3.2 MLE. In the case of the data from the 1.0 ML film there is a sharp surface peak followed by very low background, but for the higher coverages, particularly the 3.2 MLE film, distinct inelastic tails can be seen on the peaks, indicating the presence of multilayer islands of Bi, and thus of subsurface Bi atoms. The energy range of the tails is similar for the 1.8 MLE and 3.2 MLE data sets, suggesting that the average film thicknesses are similar, but the ratio of the scattered-ion intensity at 96.6 keV (directly behind the surface peak) is roughly 3 to 1; ions at this energy are scattered from subsurface atoms, so the implication is that the fractional area covered by islands has increased by this ratio. This indicates islands of a similar height cover the surface in the two preparations, but the higher-coverage sample has islands that either have a larger lateral size or a greater number density.

Figure 5 shows a plot of the variation in total intensity of ions scattered from Bi atoms as a function of scattering angle for the three different Bi coverages. For the 1.0 ML Bi sample this blocking curve is essentially featureless, as would be expected when all the atoms occupy a single layer at the surface with no additional atoms above to produce blocking dips. For the 1.8 MLE sample, the curve shows weak blocking dips at 81° and 101°. These features are more prominent in the 3.2 MLE data and broader dips at 91° and 111° can also be seen; this is consistent with an increased coverage of Bi islands. The presence of dips in the blocking curves for the islanded samples indicates that they have at least partial crystalline ordering, and that the islands have preferred crystallographic orientations relative to the Bi monolayer and the substrate below. While the amplitudes of the blocking dips seen are relatively small, this could be a consequence of the islands being oriented in multiple (symmetrically equivalent) rotational domains. For example, if the islands have a rhombohedral structure with {110} orientation (pseudocubic {001}), at least five rotational domains would be expected with the possibility of ten. It is likely that only one or two (for fivefold and tenfold symmetric surfaces, respectively) of these domains would have one of their principal crystallographic directions aligned in the scattering plane (chosen to correspond to a symmetry direction of the underlying bulk solid). In this case, the majority of the scattered-ion intensity would come from essentially random-like orientations, in which virtually complete ion illumination of the subsurface Bi atoms could be expected. Of course, an alternative potential explanation of the weak blocking dips is that the islands could have less than perfect crystallinity, since disorder leads to a reduction in dip amplitudes.

Figure 6 shows the blocking curves obtained in a similar way from the peak in the energy spectra due to scattering from the Pd substrate atoms, collected from the clean surface and from the 1.0 ML Bi sample. Differences between these data should contain information about the positions of the Bi atoms in the pseudomorphic monolayer relative to the substrate, since if they are located in well-defined adsorption sites, they will cause additional blocking dips in the signal from the substrate. This effect should occur for all three elemental components of the substrate scattering but the Pd signal is easiest to analyze for two reasons. First, Pd, as the highest mass-number atom, has the largest cross section and thus gives a high number of counts. Second, because of the higher mass, the Pd peak occurs at the highest energy of the substrate peaks, and therefore has no underlying background of inelastically scattered ions from the other substrate species. The first thing to note about the comparison of the Pd blocking curves from the clean and 1.0 ML Bi surface is that there is almost no difference between them; the blocking dips that are present have the same angular positions, the

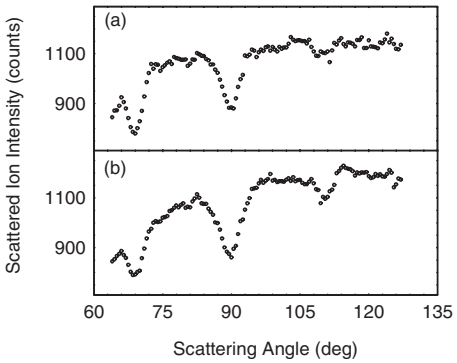

FIG. 6. Angular dependence of the scattered-ion intensity from Pd for (a) clean surface and (b) 1 MLE Bi. As in Fig. 5 the incidence angle is 31.8° and a range of in-plane scattering angles are shown. The blocking curves are essentially identical in both spectra, having the same overall intensity, blocking dip positions and amplitudes.

same depths, and the two curves have very similar overall intensity. This strongly suggests that very few of the adsorbed Bi atoms occupy well-defined sites that lie in the same azimuthal (scattering) planes as the substrate atoms. As a result, it is unlikely that the data are capable of providing a definitive description of the positions of the adsorbed atoms. However, it is still possible that certain model structures can be eliminated, since if a simulation of the substrate blocking curve for a particular model predicts large changes, this model can be rejected as inconsistent with the experimental data.

IV. ANALYSIS AND DISCUSSION

A. Structure of the pseudomorphic monolayer

In order to explore further the information which can be gained regarding the structure of the pseudomorphic monolayer, VEGAS computer simulations[23] of the MEIS substrate-scattering blocking curves were carried out for several trial structures and/or adsorption sites. The obvious starting point for this analysis is the theoretical modeling work of Krajčí and Hafner.[11,12] Figure 7(a) shows the positions of the topmost layers of the substrate for a 2/1 approximant model. A schematic illustrating the Bi atom positions on a 2/1 approximant is shown in Fig. 7(b). In this model several different types of adsorption site can be identified. There are nine sites that are located at the vertices of the Penrose P1 tiling, superimposed on the surface and in addition, 15 more half way along the edge of each tile segment. 15 more atoms are situated in pentagonal arrangements within the three pentagons seen in the tiling. The two remaining Bi atoms are located in fat rhombus and boat tiles. The fat rhombus site can be ignored since this only exists because of the use of a periodic approximant and in the real aperiodic structure it will not occur. The boat site is also ignored because only one atom occupies this site, so its effect is expected to be very small compared to that of the other three higher occupancy sites. The work of Krajčí and Hafner[11] provides a more detailed account of these various sites and the chemical environment

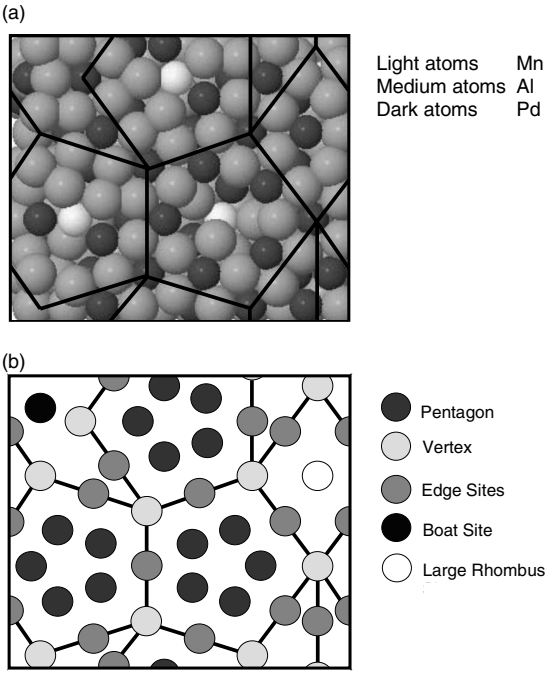

FIG. 7. (a) The 1/2 approximant model for *i*-Al-Pd-Mn showing the positions of substrate atoms relative to the Penrose P1 tiling (from Ref. 11). (b) Theoretical arrangement of Bi atoms. There are three proposed high-occupancy sites, pentagonal, edge, and vertex, along with two low-occupancy sites, boat, and large rhombus.

in the locality of each individual site. Figure 8 shows a comparison between the VEGAS simulations for the clean surface and for models with Bi atoms adsorbed in each of these three sites. The experimental data are also included in Fig. 8 for direct comparison. It is interesting to note that the amplitudes of the blocking dips seen in the data are significantly smaller than the simulations; this can be attributed to imperfect ordering in the substrate as discussed in previous MEIS studies of this surface.[22] It is evident that adsorption of Bi in either vertex or edge sites gives rise to different features in the

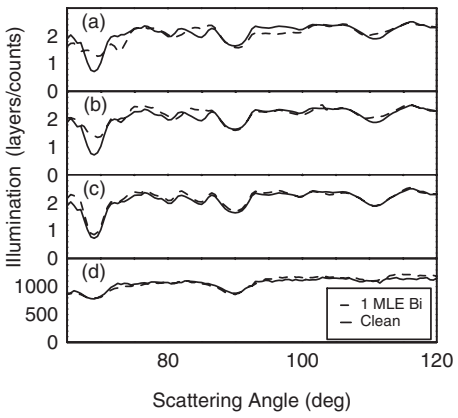

FIG. 8. VEGAS simulations of the Pd surface data for various adsorption sites on the *i*-Al-Pd-Mn surface compared with the clean surface. (a) Vertex sites, (b) edge sites, (c) pentagonal sites, and (d) experimental data. Both vertex and edge sites lead to a change in the blocking patterns whereas for pentagonal sites no change is apparent.

substrate signal which are not present in the experimental data. The MEIS analysis therefore indicates that neither of these sites has significant occupancy, despite the fact that theoretical modeling shows them to be energetically stable.[11] On the other hand the VEGAS simulations show no additional features for Bi atoms forming a pentagonal arrangement inside the P1 tiles. The reason for this is that while the atoms all occupy similar sites, only three of the 15 atoms are expected to lie in the same azimuthal scattering plane as the substrate atoms; two of these are in one orientation of the pentagon and the third atom is in the other. For this reason any effect the Bi atoms have on the blocking spectra would be expected to be very weak. The fact that the MEIS data are consistent with occupation of pentagonal features within the P1 tiles is in good agreement with recent STM work, which showed these features to form at low coverage, though only for one of the two possible orientations of the pentagonal tile.[13] From the perspective of the MEIS data, the additional Bi atoms which form the remainder of the monolayer film must sit in less well-defined sites. It would be tempting to describe these sites as a random in filling of the spaces between the pentagonal arrays that form at low coverage, but a truly random arrangement would not be consistent with the LEED/HAS study which indicated a high degree of order in the monolayer film.[5] In fact the MEIS data do not distinguish between random sites and those that are significantly out of the azimuthal planes of the substrate atoms that correspond to the scattering geometry.

Returning to the theoretical (density-functional theory) work of Kračjí and Hafner,[11,12] in a final fitting stage they allow Bi atoms to relax away from the ideal sites to minimize the surface energy. Because the atoms at the vertex sites are strongly adsorbed, they do not move significantly from the unrelaxed positions. However, the same cannot be said for the edge and pentagonal sites, which can move up to 1 Å from their starting positions and have an average movement above 0.5 Å. Since the width of the blocking cone for ions scattered from Pd at average atomic separations is approximately 0.2–0.3 Å, these relaxed positions would not give rise to any features in the blocking curves. Of course the relaxed model of Kračjí and Hafner can still be ruled out because it requires atoms to be present at vertex sites, which is inconsistent with the MEIS data.

Another potential model for the pseudomorphic monolayer is a continuation of the bulk structure. However, this model can be easily rejected on similar grounds to the edge and vertex sites previously discussed, since it would give rise to significant changes in the Pd-surface blocking curve. Modeling of this effect can be achieved by substituting the surface layer of atoms for those of the adsorbate. While no relevant simulations are shown here, an example can be seen in Fig. 6 of Ref. 10, where a similar calculation is presented for Au atoms on the fivefold *i*-Al-Pd-Mn surface. Essentially, the addition of heavy adsorbate atoms on lattice sites causes the blocking dips to deepen and widen, but neither of these effects can be seen in the data.

B. Size distribution of Bi islands at higher coverage

The energy spectra for the three Bi coverages shown in Fig. 4 have been fitted using an energy simulation code developed for use with islanded overlayers.[24] In this code the quality of theory/experiment agreement is assessed using a reliability factor (*R* factor). Fitting of the 1.0 ML data was first used to determine the values of the nonstructural parameters, namely, resolution, calibration, and peak shape asymmetry; Ref. 25 provides a discussion of the importance of peak shape in fitting spectra of this type. A reasonably good fit could be achieved to the higher coverage data sets using islands with a thickness of 4 atomic layers (AL) and fractional coverages of 20% and 56% for the samples with average Bi coverages of 1.8 MLE and 3.2 MLE, respectively. However, a significant reduction in the *R* factor (by about 15%) could be gained by adopting a model involving a mixture of islands with thicknesses of 2, 4, 6, and 8 AL. The excellent fits achieved to all the data sets using this procedure suggest that the results, in terms of island height distribution, are reliable.

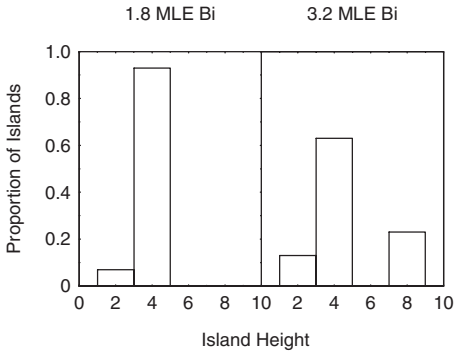

FIG. 9. A bar chart of island height distributions for 1.8 and 3.2 MLE coverages of Bi. Multiples of 4 AL island heights are clearly favored and it is notable that no 6 AL islands are present for either coverage.

Figure 9 shows a plot of the island height distribution for the 1.8 and 3.2 MLE coverage data sets. For the 1.8 MLE data, the vast majority of the islanded Bi is present as 4 AL islands with the remainder in 2 AL islands. For the 3.2 MLE data set, the majority of islanded Bi is also in 4 AL islands, but in this case the fit reveals some occupation of 2 AL and 8 AL islands as well. The presence of some thicker islands for the higher coverage might be expected but the greater amount of 2 AL islands at higher coverage is more surprising. However, this may be a consequence of the data collection being carried out more rapidly for this sample than for the 1.8 MLE sample. Previous STM results identified a considerable number of 2 AL islands on the surface just after deposition but these were found to erode over the course of an hour or so to form mostly 4 AL islands.[15] It is interesting to note that neither fit finds any occupation of 6 AL islands. The data are therefore consistent with the preference for multiples of 4 AL island heights as suggested in the earlier STM studies of Bi on *i*-Al-Cu-Fe (Ref. 15) and Bi on Al-Pd-Mn.[14]

The presence of multiples of 4 AL islands rather than 2 AL islands might suggest that the origin of these islands is related to quantum size effects as stated in the original work.[15] However, the fact that only even numbers of layers are preferred may indicate that another relevant factor is the formation of a bilayer type of structure, as reported for Bi

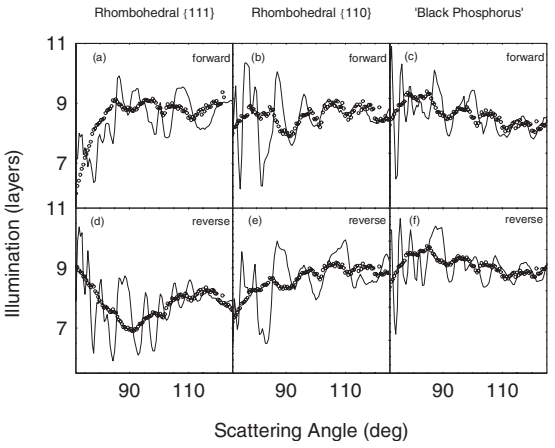

FIG. 10. Various structural models for the Bi clusters tested against the data. The forward direction is along the Y azimuth shown in Fig. 10 and the reverse direction is rotated by 180° (the simulations are averages including components at angles of 72° and 144° away from these directions to account for the five rotational domains). The simulations presented in (a) and (d)–(f) do not compare favorably with the data, but those in (b) and (c) show some similarity, particularly for scattering angles below 90° where both the position and amplitude of blocking dips coincide.

growth on Si (111).[17,18] An investigation of the structure of the Bi islands was therefore carried out.

C. Structure of the Bi islands

In order to ascertain the structure of the Bi islands, VEGAS simulations of various trial structures were compared with the experimental blocking curves. For this purpose only the higher coverage 3.2 MLE data were used, since these show stronger blocking features, as seen in Fig. 5. Following the conclusions of the previous studies of Bi on *i*-Al-Cu-Fe (Ref. 15) and Si(111) (Refs. 17 and 18) the trial structures used were based on the bulk structure of Bi with either rhombohedral {110} (pseudocubic {100}) or rhombohedral {111} (pseudocubic {111}) orientations to the surface. In addition, a puckered black-phosphoruslike structure, which is essentially a distortion of the pseudocubic {100} to form bilayers, was also modeled. Multiple simulations were run and averaged for each structure to account for the presence of rotational domains. The search focused primarily on models having five rotational domains, since this is consistent with the symmetry seen with RHEED for Bi islands on *i*-Al-Cu-Fe.[15] Some evaluation of more obvious models with tenfold symmetry was also carried out. This was by no means exhaustive, because of the many possible models, but none of the tenfold models evaluated gave good agreement with the data.

Figure 10 shows a comparison of the experimental data with the results of the simulations for the three different fivefold model structures, each in two different rotational orientations. Two different orientations of the film have been modeled, both of which involve the alignment of the twofold axis of the islands with the fivefold axis of the substrate. The first of these, described as "normal" in Fig. 10 is shown in Fig. 11. The second, which is described as "reversed" has the

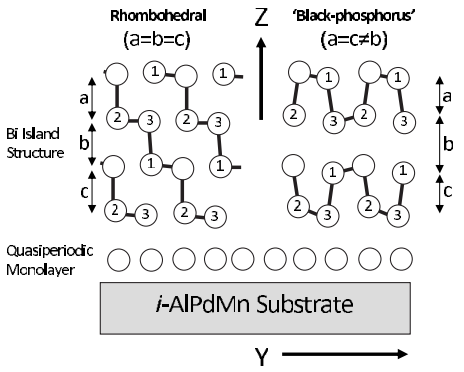

FIG. 11. Structural models for rhombohedral and black-phosphoruslike Bi islands. A large downward shift in the positions of the atoms marked "1" from their positions in the rhombohedral structure leads to the formation of bilayers in the islands.

film rotated by 180° with respect to the first. These two orientations are the only ones allowed which would give rise to five rotational domains. The closest agreement with the experimental data is achieved with the model labeled as normal for the rhombohedral {110} (pseudocubic {100}) model and with the closely related black-phosphorouslike model. The similarity of the blocking curves for these two models is to be expected, because the structures are closely related, as shown in Fig. 11, differing only by small shifts in the lateral and vertical positions of the atoms. These two models were therefore used as a starting point for further investigation of the island structure.

As is clear from Fig. 10, the agreement between simulation and experiment is much better at higher scattering angles than at low angles. This can be attributed to the fact that the simulations have been carried out using models that are continuous films of each structure whereas the data come from islands with finite lateral dimensions. At low-scattering angles a range of long scattering paths are possible within a continuous film, but many of these cannot occur, or are rare, in islands of limited lateral size. The simulations thus give rise to a number of intense blocking dips at low angle that are unlikely to be present in the experimental data. In order to avoid this problem, two measures were taken in subsequent fitting of the data. The first was to use more realistic models with islands of finite size. This is possible using the VEGAS simulation code, but it does add significantly to the computation time. Figure 12 shows a comparison of the simulated blocking curves for a single domain of a continuous film, and for an islanded model; a significant reduction in the number and intensity of blocking dips at low-scattering angles can be clearly observed for the islanded model. Modeling an island structure can only be achieved by using much larger clusters of atoms, and as the computation time scales with the number of atoms, this becomes a very challenging problem. Further calculations were carried out using 25×25 Å^2 islands in a 100×100 Å^2 box, consistent with the STM images for Bi on *i*-Al-Cu-Fe (Ref. 15) and Bi on *i*-Al-Pd-Mn.[14] In these calculations, a more limited range of scattering angles was used in the analysis, excluding some of the low-angle data that are likely to be most dependent on the precise island size and shape distribution. Fitting of these

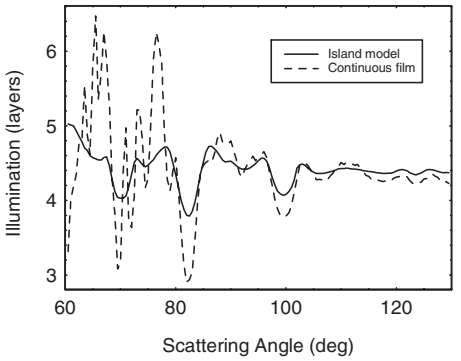

FIG. 12. A comparison of the simulated spectra of a single domain of rhombohedral Bi, for a continuous film and an islanded structure. The differences between simulations become particularly pronounced at low-scattering angle.

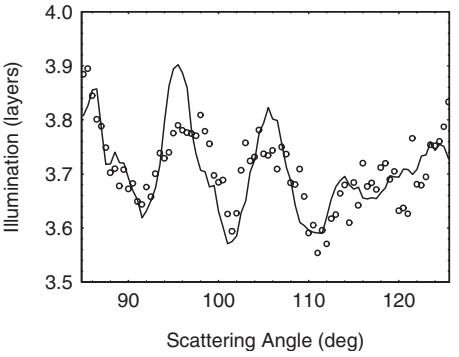

FIG. 13. Best fit between simulation and data for the Bi island structure. The structure is essentially like the rhombohedral {110} model [Fig. 9(b)] but with the topmost atoms in each bilayer shifted down by 0.79 Å.

morphological parameters is not possible in current versions of the analysis code.

Fitting of the island models was carried out using an auto-optimization routine incorporating the VEGAS code, and a χ^2 reliability factor to compare the simulations with the data. This code typically needs to run many simulations (over a hundred in this instance) before finding the optimum solution. Coupled with the large model size, this task only proved achievable with the development of a multithreaded version of the code, written to exploit a computer having many parallel processor cores (in this case 16). The development of a multithreaded auto-optimization code is an important step in the analysis of MEIS blocking curves from nanostructured surfaces.

The auto-optimization used, as the initial starting structure, the pseudocubic {100} model, and allowed atoms to relax both parallel and perpendicular to the film, allowing the possibility of converging on the puckered "black-phosphorous" structure. The relative positions of the atoms in the first and second layers were initially assumed to be the same as those of the third and fourth layers in order to minimize the number of parameters. The best fit between the experimental data and the simulation is shown in Fig. 13 while the associated structural parameter values are listed in Table I. The fit between the data and simulation is generally good, despite the relatively poor signal-to-noise ratio of the experimental data. In particular, the magnitudes of the dips are reproduced well, indicating a high degree of crystalline order within the islands. The structural parameter values listed indicate small movements for a number of atoms but most of these are no larger than the estimated errors in the determination. The notable exception is the very large and statistically significant perpendicular movement of the outermost atom into the film, and its partner in the third layer, by 0.78 Å. The importance of this movement is that it effectively leads to bilayer formation within the film, since the separation of layers 1 to 2, and of layers 3 to 4, is now significantly smaller than the separation of layers 2 to 3 (Fig. 11).

One potential problem with this fitting procedure in which the displacements of the atoms with the top two layers are linked to those in the bottom two, is that a film with a significant inward relaxation of the surface atoms alone could be misinterpreted as bilayer formation. For this reason, in a further test, the other optimized parameters were held constant and the perpendicular displacements of the two atoms which lead to bilayer formation in the top and third layers (both marked 1 in Fig. 11), were allowed to vary independently. As shown in the final column of Table I, the optimal positions of both atoms still show large statistically significant inward displacements. In fact, the atom in the third layer has a larger displacement (0.77 Å) than that at the surface (0.46 Å) and of course it is this third layer atom that is critical in determining that bilayer formation has occurred.

While the structural data discussed above clearly demonstrate that bilayer formation occurs in this system, this effect

TABLE I. Atomic positions for the best-fit model relative to the rhombohedral {110} model. The suffixes of the Z and Y shifts relate to the numbered atoms in Fig. 10.

	Optimized atom positions relative to the rhombohedral {110} model	Heights of top most atoms in each bilayer when independently varied
ΔZ_1	-0.78 ± 0.52 Å	Top: -0.46 ± 0.10 Å, bottom: -0.77 ± 0.51 Å
ΔY_1	-0.07 ± 0.31 Å	
ΔZ_2	0.04 ± 0.47 Å	
ΔY_2	-0.10 ± 0.25 Å	
ΔZ_3	0.38 ± 0.70 Å	
ΔY_3	0.22 ± 0.33 Å	

alone cannot account for the height distributions seen in both MEIS and STM for Bi islands on this type of substrate. If bilayer formation were the only effect responsible, a significant fraction of islands having 6 AL would also be expected to occur, particularly at the higher of the two coverages investigated here. The most obvious additional factor that might be responsible would be quantum size effects, such as those seen for Ag on *d*-Al-Ni-Co.[16] However, Bi is only a semi-metal in its native rhombohedral state, and for the black-phosphoruslike phase, both theoretical calculations and scanning tunneling spectroscopy measurements of similar Bi clusters on Si(111) indicate a reduction in the local density of states at the Fermi level, leading to reduced metallic nature in the islands.[17] Clearly, the islands must retain some metallic character for quantum well states to occur. Ultimately, in order to refute or confirm the existence of such states, experiments such as the photoemission measurements in the previous study of Ag on *d*-Al-Ni-Co are needed. Despite this, quantum size effects, though speculative, remain the best potential explanation of the preference for 4 AL high islands seen in previous work and again in this study.

V. CONCLUSIONS

The technique of MEIS has been used to study monolayer films and multilayer islands of Bi on *i*-Al-Pd-Mn. The precise structure of the monolayer film could not be determined because no different features were seen in the MEIS blocking dips. However, several adsorption sites could be discounted as inconsistent with the experimental results. By contrast, pentagonal clusters of Bi atoms sitting inside the large pentagons of the P1 tiling were not incompatible with the MEIS data. Above 1 MLE, islands were seen that showed a preference for multiples of 4 AL height, regardless of coverage. MEIS blocking curves obtained from the Bi islands indicate that they were well ordered and were structurally similar to rhombohedral Bi with five-domain rhombohedral {110} (pseudocubic {100}) orientation but with a puckering that involved the formation of distinct bilayers in the island structure.

ACKNOWLEDGMENTS

The authors would like to thank EPSRC for funding this work under Grant No. GR/S19080/01 and for direct access to the MEIS facility under Grant No, GR/R88809/01. The FOM institute, Amsterdam is thanked for providing the VEGAS code and Paul Quinn of DLS Ltd. for providing the energy simulation software. Marian Krajčí is thanked for providing the 2/1 approximant structural model used in the simulations.

*Corresponding author; tim.noakes@stfc.ac.uk

[1] V. Fournée and P. A. Thiel, J. Phys. D **38**, R83 (2005).
[2] R. McGrath, J. A. Smerdon, H. R. Sharma, W. Theis, and J. Ledieu, J. Phys.: Condens. Matter **22**, 084022 (2010).
[3] V. Fournée, T. C. Cai, A. R. Ross, T. A. Lograsso, J. W. Evans, and P. A. Thiel, Phys. Rev. B **67**, 033406 (2003).
[4] T. Cai, J. Ledieu, R. McGrath, V. Fournee, T. A. Lograsso, A. R. Ross, and P. A. Thiel, Surf. Sci. **526**, 115 (2003).
[5] K. J. Franke, H. R. Sharma, W. Theis, P. Gille, P. Ebert, and K. H. Rieder, Phys. Rev. Lett. **89**, 156104 (2002).
[6] H. R. Sharma, M. Shimoda, J. A. Barrow, A. R. Ross, T. A. Lograsso, and A. P. Tsai, *Quasicrystals 2003 - Preparation, Properties and Applications*, MRS Symposia Proceedings No. 805 (Materials Research Society, Pittsburgh, 2004).
[7] J. Ledieu, J. T. Hoeft, D. E. Reid, J. A. Smerdon, R. D. Diehl, T. A. Lograsso, A. R. Ross, and R. McGrath, Phys. Rev. Lett. **92**, 135507 (2004).
[8] J. A. Smerdon, J. Ledieu, R. McGrath, T. C. Q. Noakes, P. Bailey, M. Draxler, C. F. McConville, T. A. Lograsso, and A. R. Ross, Phys. Rev. B **74**, 035429 (2006).
[9] M. Shimoda, J. Guo, T. J. Sato, and A. P. Tsai, Jpn. J. Appl. Phys., Part 1 **40**, 6073 (2001).
[10] T. C. Q. Noakes, P. Bailey, M. Draxler, C. F. McConville, A. R. Ross, T. A. Lograsso, L. Leung, J. A. Smerdon, and R. McGrath, J. Phys.: Condens. Matter **18**, 5017 (2006).
[11] M. Krajčí and J. Hafner, Phys. Rev. B **71**, 184207 (2005).
[12] M. Krajčí and J. Hafner, Philos. Mag. **86**, 825 (2006).
[13] J. A. Smerdon, J. K. Parle, L. H. Wearing, T. A. Lograsso, A. R. Ross, and R. McGrath, Phys. Rev. B **78**, 075407 (2008).
[14] H. R. Sharma, V. Fournée, M. Shimoda, A. R. Ross, T. A. Lograsso, P. Gille, and A. P. Tsai, Phys. Rev. B **78**, 155416 (2008).
[15] V. Fournée, H. R. Sharma, M. Shimoda, A. P. Tsai, B. Unal, A. R. Ross, T. A. Lograsso, and P. A. Thiel, Phys. Rev. Lett. **95**, 155504 (2005).
[16] P. Moras, Y. Weisskopf, J. N. Longchamp, M. Erbudak, P. H. Zhou, L. Ferrari, and C. Carbone, Phys. Rev. B **74**, 121405(R) (2006).
[17] T. Nagao, J. T. Sadowski, M. Saito, S. Yaginuma, Y. Fujikawa, T. Kogure, T. Ohno, Y. Hasegawa, S. Hasegawa, and T. Sakurai, Phys. Rev. Lett. **93**, 105501 (2004).
[18] T. Nagao, S. Yaginuma, M. Saito, T. Kogure, J. T. Sadowski, T. Ohno, S. Hasegawa, and T. Sakurai, Surf. Sci. **590**, 247 (2005).
[19] P. Bailey, T. C. Q. Noakes, and D. P. Woodruff, Surf. Sci. **426**, 358 (1999).
[20] J. Ledieu, A. W. Munz, T. M. Parker, R. McGrath, R. D. Diehl, D. W. Delaney, and T. A. Lograsso, Surf. Sci. **433-435**, 666 (1999).
[21] M. Mayer, Max-Planck-Institute fur Plasmaphysik "SIMNRA User's Guide" Report No. IPP 9/113, 1997.
[22] T. C. Q. Noakes, P. Bailey, C. F. McConville, C. R. Parkinson, M. Draxler, J. Smerdon, J. Ledieu, R. McGrath, A. R. Ross, and T. A. Lograsso, Surf. Sci. **583**, 139 (2005).
[23] J. F. Frenken, J. F. van der Veen, and R. M. Tromp, Nucl. Instrum. Methods Phys. Res. B **17**, 334 (1986).
[24] P. D. Quinn, N. R. Wilson, S. A. Hatfield, C. F. McConville, G. R. Bell, T. C. Q. Noakes, P. Bailey, S. Al-Harthi, and F. Gard, Appl. Phys. Lett. **87**, 153110 (2005).
[25] P. L. Grande, A. Hentz, R. P. Pezzi, I. J. R. Baumvol, and G. Schiweitz, Nucl. Instrum. Methods Phys. Res. B **256**, 92 (2007).